Splitting in the excitation spectrum of a Bose-Einstein condensate undergoing strong Rabi oscillations

E. Rowen, R. Ozeri, N. Katz, E. Gershnabel, and N. Davidson
Department of Physics of Complex Systems, Weizmann Institute of Science, Rehovot 76100, Israel
(Received 23 June 2005; published 15 November 2005)

We report on a measurement of splitting in the excitation spectrum of a condensate driven by an optical traveling wave. Experimental results are compared to a numerical solution of the Gross-Pitaevskii equation, and analyzed by a simple two-level model and by the more complete band theory, treating the driving beams as an optical lattice. In this picture, the splitting is a manifestation of the energy gap between neighboring bands that opens on the boundary of the Brillouin zone.

DOI: 10.1103/PhysRevA.72.053614 PACS number(s): 03.75.Lm, 03.75.Kk, 32.80.−t

Perturbative bulk excitations over the ground state of a weakly interacting Bose Einstein condensate (BEC) have been extensively studied using two-photon Bragg transitions [1–4]. Their spectrum [5], dynamics [6], and decay [7] are rather well understood. However, Bragg processes can also strongly excite the condensate, generating nonperturbative dynamics, such as Rabi oscillations between two (or more) macroscopically populated momentum states [8–10]. Rapid oscillations have been found to suppress various inhomogeneous broadening mechanisms, thus increasing the coherence time of the system [9].

Since the Bragg process may be viewed as the diffraction of an atomic wave packet from a nearly perfect optical lattice, band theory may be employed for the study of such systems. A BEC in an optical lattice has proved to be an excellent system for the investigation of effects predicted long ago in solid state physics such as Bloch oscillations and Landau-Zener intraband tunneling [8,11–13], and the Mott-insulator phase transition [14]. Much progress has been made in understanding the ground state of a BEC in an optical lattice, its weak excitations, and the effects of interactions [15,16]. However strong excitations involve two beating macroscopically occupied modes, and lead to Rabi-like oscillations. Thus they cannot be described as a Bogoliubov-like excitation over a single Bloch state.

In this paper we study the spectrum of a BEC driven by a strong resonant Bragg pulse, which leads to coherent Rabi oscillations between momentum states. We observe these oscillations in the time domain and a splitting between the energy bands in the frequency domain. The splitting is measured experimentally with Bragg spectroscopy, using an additional Bragg beam pair as a weak probe, and found to agree with numerical solution of the time-dependent Gross-Pitaevskii equation (GPE). The splitting is also predicted by a simplified two-level dressed-state model. However some features are explained only by the more complete band theory. These theories do not include inhomogeneous and finite-size effects, nor interactions, but are in reasonable agreement with our experimental results.

The energy spectrum of a linear system is related to the time dynamics via Fourier transform. Therefore the oscillations in the time domain are translated to splitting in the spectrum, and the decay of the time-correlation function results in broadening of the spectral peaks [17]. In our experiment the chemical potential, which characterizes the nonlinearity, is smaller than the Rabi frequency, but of the same order of magnitude. Hence this linear description is only approximately true for our system.

Our experimental apparatus is described in [5]. Briefly, a nearly pure (~90%) BEC of $(5\pm1)\times10^4$ ^{87}Rb atoms in the $|F,m_f\rangle=|2,2\rangle$ ground state, is formed in a magnetic trap with radial and axial trapping frequencies of $\omega_r=2\pi\times226$ Hz and $\omega_z=2\pi\times26.5$ Hz, respectively. The condensate is driven by a pair of strong counterpropagating Bragg beams with wave vectors $k_L\hat{z}$ and $-k_L\hat{z}$ generating an optical lattice potential along the axial direction with a depth characterized by a Rabi frequency Ω_d. The laser frequency is red detuned 44 GHz from the ^{87}Rb D_2 transition in order to avoid spontaneous emission. As shown in [9], in the Rabi regime the mean-field shift is largely suppressed, hence the frequency difference between the driving Bragg beams (in the laboratory frame) is set to $\omega_d=2\pi\times15$ kHz, the free-particle resonance.

After driving pulses of varying duration, the magnetic

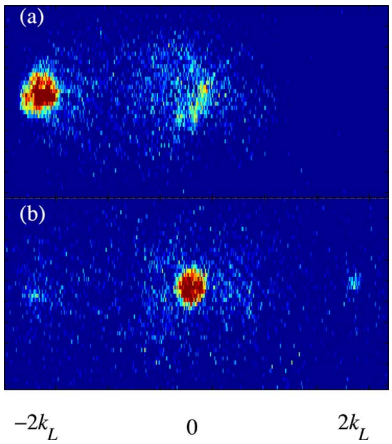

FIG. 1. (Color online) Time-of-flight images of BEC undergoing strong Rabi oscillations. (a) BEC evolved in the presence of driving Bragg beams alone. The pulse of duration 320 μs is just over $3\pi/\Omega_d$, leaving almost all population in $-2k_L$ momentum state. (b) Both driving Bragg beams and probe Bragg beams are on for 600 μs. Driving pulse is close to $6\pi/\Omega_d$ leaving the state $-2k_L$ almost unoccupied.

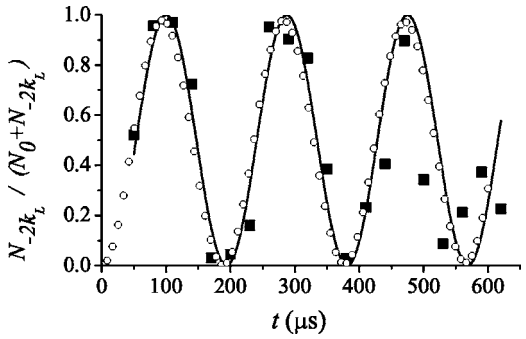

FIG. 2. Rabi oscillations between modes with wave numbers 0 and $-2k_L$ (in the laboratory frame of reference). The solid line is a sinusoidal fit to the data which gives an oscillation frequency of $2\pi\times 5.34$ kHz. The open circles are the GPE simulation with $\Omega_d=2\pi\times 5.5$ kHz whose sinusoidal fit gives the same oscillation frequency. The oscillation frequency is less than Ω_d due to interactions, which in effect lower the depth of the optical lattice.

trap is rapidly turned off. A typical absorption image after 38 ms time-of-flight expansion is shown in Fig. 1(a). The wave packets with wave number $-2k_L$ and $k=0$ are clearly separated. In this image, $\Omega_d t\sim 3\pi$, hence most atoms are in the $-2k_L$ wave packet. The number of atoms in each wave packet is measured by integration over the density in an area determined by a Gaussian fit to the absorption image. We thus define N_{-2k_L} and N_0 as the number of atoms in the wave packets with wave numbers $-2k_L$ and 0, respectively.

Figure 2 shows the time dynamics of the BEC exposed to the driving Bragg beams. The solid squares are data points, measuring the fraction of atoms in $-2k_L$ cloud as a function of the duration of the driving pulse. The BEC undergoes oscillations at a frequency of $2\pi\times(5.3\pm 0.1)$ kHz as found from a sinusoidal fit to data. The hollow points are numerical solutions of the GPE including finite time and spatial inhomogeneity with Ω_d as the only fit parameter [18]. The Rabi frequency that yields the correct oscillation frequency is found to be $\Omega_d=2\pi\times 5.5$ kHz. The oscillation frequency is slightly less than Ω_d due to interactions. This is because the higher density in the valleys of the optical potential creates a mean-field lattice potential opposing the optical one [11,16].

Next, we probe the spectrum of the oscillating BEC, with another pair of Bragg beams (turned on simultaneously with the driving Bragg beams), generating a weak lattice with a Rabi frequency Ω_p. The probe beams, also counterpropagating along the axial direction, are linearly polarized perpendicular to the driving beams. The frequency difference between probe beams ω_p is always kept such that the zero-momentum wave packet is diffracted by the probe lattice to a $2k_L$-momentum wave packet, whereas for the $-2k_L$ wave packet, the Bragg frequency of the probe beams is always Doppler shifted away from resonance. For the same reason, the driving beams are Doppler shifted from the $2k_L$ state. A characteristic time-of-flight image is shown in Fig. 1(b). Here in addition to the clouds in states $-2k_L$ and 0, there are also atoms with wave number $2k_L$. The measured relative population of this momentum state $N_{2k_L}/(N_{-2k_L}+N_0+N_{2k_L})$ as a function of the probe frequency difference ω_p forms the probe Bragg spectrum, which is plotted in Fig. 3 (black

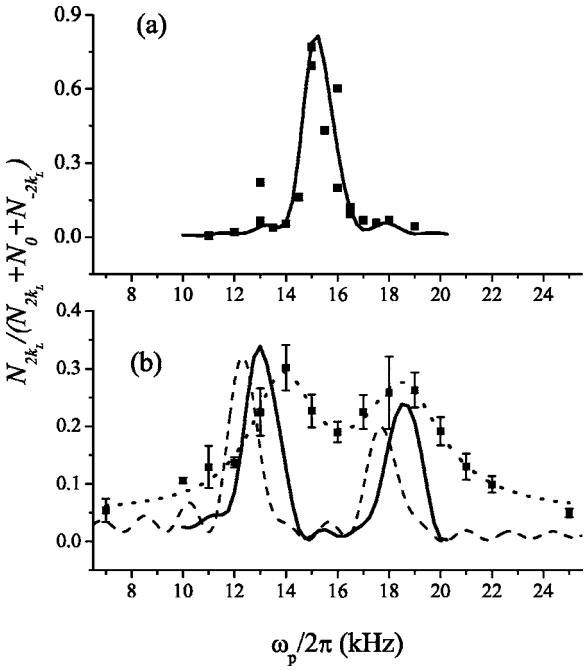

FIG. 3. Excitation spectra: Fraction of atoms in $2k_L$ state as a function of the probe frequency difference. (a) No lattice ($\Omega_d=0$) and (b) $\Omega_d=5.5$ kHz. In (a) the solid line is a GPE simulation with Ω_p as a single free parameter. In (b) the solid line is a GPE simulation with Ω_p the same as in (a), and Ω_d determined by Fig. 2. The dotted line is a Lorentzian fit to the data giving a splitting of $\Delta E=h\times(4.7\pm 0.2)$ kHz. The dashed line is the noninteracting band model discussed in the text.

squares). The duration of the beams is set so the driving pulse will be close to an even multiple of π, in order to minimize collisions in the time-of-flight expansion.

The probe spectrum without the driving beams ($\Omega_d=0$) is similar to the well-known Bogoliubov spectrum [Fig. 3(a)]. The probe is weak in the sense that $\Omega_p\simeq\Omega_d/8$, but since the probe pulse is greater than $\pi/2$ we observe a suppression in the mean-field shift [9]. The probe spectrum in the presence of the driving beams [Fig. 3(b)] shows a clear splitting in the spectrum of the oscillating condensate. The dotted line is a double-Lorentzian fit to the experimental data, with a distance between the peaks of $\Delta E/h=4.7\pm 0.2$ kHz, comparable to but larger than the chemical potential $\mu/h=1.6$ kHz. The solid line is the full GPE simulation of the experiment, which gives a splitting of $\Delta E/h=5.5$ kHz. We note this is not the frequency of oscillations in Fig. 2, but rather the Rabi frequency of the lattice itself. The mismatch between experimental and simulation results, is probably due to a drift in the intensity and the detuning of the laser. This drift is estimated to cause a 10–20 % drift in the Rabi frequency.

The width of the spectrum without driving [Fig. 3(a)] fits the GPE simulation, and is mostly due to the finite time of the experiment. However, the experimental peaks in Fig. 3(b) are substantially broader than predicted by the GPE. This broadening is robust and is observed for different values of Ω_d, indicating broadening mechanisms which are beyond mean field. One such mechanism for a homogeneous condensate is due to uncertainty in the dressed-state decomposi-

tion of the initial Fock state, which leads to a spectral broadening [19]. For our experimental parameters this broadening is much less than the widths of the experimental peaks, which are 3 ± 0.4 and 3.7 ± 0.5 kHz. The 0.5–1 kHz drift in the Rabi frequency cannot account for the much larger broadening of the peaks. We do not quantitatively understand the broadening. The overall response of the system to the probe is smaller in Fig. 3(b) (with driving beams) than that in Fig. 3(a) (without driving beams). This is because the time-averaged population of the state $k=0$ in the presence of the lattice is only half of that of the ground state of the BEC.

The simplest model that explains the splitting in the spectrum is a noninteracting model of a closed system with two momentum states: 0 and $-2\hbar k_L$, coupled to a classical light potential. Choosing our frame of reference as moving with the optical lattice of the Bragg driving beams at velocity $v=-k_L/M$ along z yields a time-independent Hamiltonian,

$$H_0 = -\frac{\hbar^2}{2M}\frac{\partial^2}{\partial z^2} + \hbar\Omega_d \cos(2k_L z). \tag{1}$$

The eigenstates of such a Hamiltonian are dressed states [20]. The energy difference between the two eigenenenergies is $\hbar\Omega_d$. This energy difference is manifested both in the splitting of the spectrum and in the Rabi oscillations, which are the coherent beating between the two eigenstates. Since the initial $k=0$ state is an equal superposition of the two dressed states, the two peaks in the spectrum are expected to have the same heights.

The system is, however, not a closed two-state system, as there are nonresonant Rabi oscillations with other momentum states. We therefore calculate the eigenstates of the noninteracting Hamiltonian (1) without the restriction to two momentum states. According to Bloch's theorem, due to the periodicity of the optical lattice, a state $|k\rangle$ with wave number k is coupled only to states $|k+2mk_L\rangle$, where m is an integer, and $2k_L$ is the basis of the reciprocal lattice. The Hamiltonian is diagonalized by the Bloch states

$$|n,q\rangle = \sum_m a_{n,q}(k)|q+2mk_L\rangle \tag{2}$$

where q is the *quasimomentum* and n is the band index [2]. In the moving frame of reference, the stationary BEC has momentum $\hbar k_L$ and is situated on the Brillouin zone boundary. The initial kinetic energy of the condensate is in the energy gap, and by suddenly turning on the light potential, the initial state $|k_L\rangle$ is projected onto the Bloch states $|k_L\rangle=\Sigma_n a_n(k_L)|n\rangle$, where we have omitted the quantum number q which is understood to be $q=k_L$.

In the weak-lattice limit, $\hbar\Omega_d \ll E_r$ where $E_r=\hbar^2k_L^2/2M$ is the single-photon recoil energy, we recover the two-state result $|k_L\rangle=1/\sqrt{2}(|1\rangle+|2\rangle)$, and a splitting of Ω_d. For our parameters the band structure is obtained by numerical diagonalization and presented in Fig. 4. The predicted splitting between the two lowest bands is indeed within 1% of Ω_d, but contrary to the weak-lattice approximation, $|a_3(\pm k_L)| = |a_4(\pm k_L)| \approx 10\%$ of $|a_3(\pm 3k_L)| = |a_4(\pm 3k_L)|$. This indeed leads to negligible occupations, but as we show shortly, to observable interference effects.

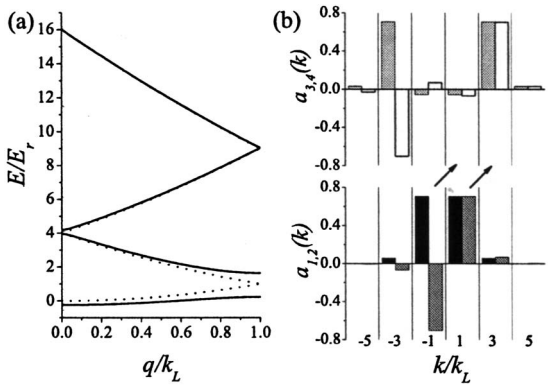

FIG. 4. Noninteracting band structure for our experimental parameters. (a) The energy of the four lowest bands as a function of quasimomentum (solid lines). The energy gap on the boundary of the Brillouin zone is $0.99\ \hbar\Omega_d$, while the gap between the third and fourth bands is two orders of magnitude smaller. The dashed line is the free-particle energy. (b) The amplitudes of the different momentum states $k=k_L+2mk_L$ in each Bloch state on the boundary of the Brillouin zone. Black, dark gray, light gray, and white are bands 1, 2, 3, and 4, respectively. The arrows represent the coupling by the probe. Note the contamination of each Bloch state by the "unintuitive" momentum states.

With the probe beams, the Hamiltonian governing the model homogeneous system in the driving lattice frame is $H=H_0+H_p$ with

$$H_p = \hbar\Omega_p \cos(2k_L z - \omega_p t) = V_p e^{-i\omega_p t} + \text{c.c.} \tag{3}$$

with $V_p=\hbar\Omega_p e^{2ik_L z}/2$. In the rotating-wave approximation H_p is a momentum shift operator coupling state $|k\rangle$ to $|k+2k_L\rangle$. Since $\Omega_p \ll \Omega_d$, it can be treated by the use of first-order time-dependent perturbation theory, giving probability amplitudes for transitions between bands. The momentum transferred to the condensate by the redistribution of photons in the probe beams is a multiple of the reciprocal lattice vector $2k_L$; hence also with the probe beams the initial quasimomentum $q=k_L$ is conserved.

The dashed line in Fig. 3(b) is the full first-order perturbation theory expectation of the population of state $|3k_L\rangle$ in the moving frame of reference, which is equal to $2k_L$ in the laboratory frame of reference. Aside from a mean-field shift, this simple model seems to fit the GPE simulation quite well.

Since the splitting between bands 3 and 4 is negligible, the splitting in the spectrum of the probe in this noninteracting model is essentially the splitting between the two lowest bands [see Fig. 4(a)].

There is a clear asymmetry in the peak heights of the noninteracting model [dashed line in Fig. 3(b)], which is in good agreement with the GPE simulation. This asymmetry is due to quantum interferences between pathways of the probe excitation. The probe couples each of the lower bands (1 and 2) to each of the higher bands (3 and 4) by two paths. In the weak-lattice approximation there is only the path $|k_L\rangle \rightarrow |3k_L\rangle$; however due to the nonvanishing $a_3(k_L)$ and $a_4(k_L)$, there is also a path $|-k_L\rangle \rightarrow |k_L\rangle$. These paths are marked by arrows connecting the relevant amplitudes in Fig.

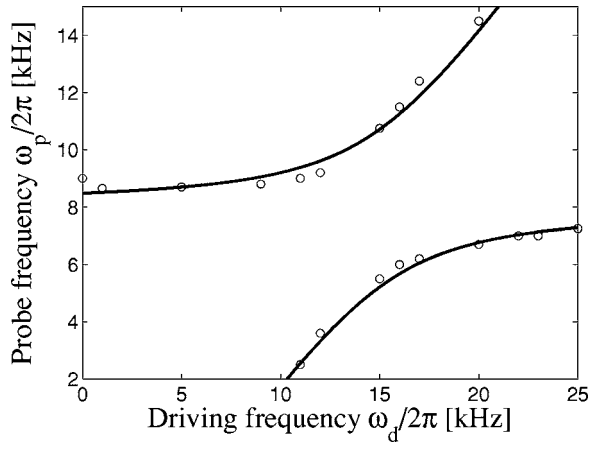

FIG. 5. The locations of the peaks in the response to the probe, as a function of the driving beams' frequency difference ω_d. Numerical solution of the GPE including finite-size, finite-time, and mean-field effects (circles), and the energy levels of a two-level system shifted up by 1.3 kHz (lines). The probe wave numbers are taken as $\pm k_L/3$ to distinguish probe excitations from nonresonant driving excitations.

4(b). The interference between both paths is constructive for transitions from band 2 and destructive for transitions from band 1. Therefore the lower-energy peak in the splitting, corresponding to transitions from band 2 should be larger than the higher-energy peak, which corresponds to transitions from band 1.

In the experiment, the frequency difference between the driving Bragg beams is equal to the free-particle resonance $\hbar\omega_d = 4E_R$. For other values of $\hbar\omega_d$, the Rabi oscillations are not full. As the detuning from resonance grows, the amplitude of oscillations is reduced and the frequency of oscillations grows. In the spectral domain the frequency difference between the two peaks of Fig. 3(b) grow with the detuning from resonance. The amplitude of one peak grows while its position in frequency shifts toward the excitation energy of a free Bogoliubov quasiparticle. The other peak shrinks in size as the detuning of ω_d from resonance grows. In Fig. 5 we plot the values of ω_p at the peak of the spectrum versus ω_d, as obtained by numerically solving the GPE [18] for $\Omega_d = 5.5$ kHz. We compare this to the energy splitting of a noninteracting two-level system, calculated for the same parameters, and shifted up by 1.3 kHz. As in the resonant case, the splitting is in good agreement with the GPE, except for a constant shift due to interactions. The mean-field shift for a Bogoliubov excitation using a local density approximation is 1.6 kHz [1]. Since our probed system is not a stationary condensate, the shift is somewhat smaller.

In conclusion, we measure a splitting in the Bragg excitation spectrum of a BEC undergoing Rabi oscillations between two momentum states. The experimental data fit well with numerical GPE simulations. The main features are captured by a simple noninteracting model, whereas the main contribution of interactions is found to be the mean field shift of the probe spectrum, captured by the GPE, and an increase in the width which is not captured by the GPE. The splitting in the spectrum results in a splitting in the energy of the atoms undergoing incoherent collisions. Experimentally, a divergence from the known s-wave scattering halo was measured for a rapidly oscillating BEC. There too, a pronounced asymmetry was found between the inner collisional shell and the outer one.

This work was supported in part by the Israel Ministry of Science, the DIP foundation, the Israel Science Foundation, and the Minerva foundation.

[1] F. Zambelli *et al.*, Phys. Rev. A **61**, 063608 (2000).
[2] P. B. Blakie and R. J. Ballagh, J. Phys. B **33**, 3961 (2000).
[3] J. Stenger *et al.*, Phys. Rev. Lett. **82**, 4569 (1999).
[4] D. Stamper-Kurn *et al.*, Phys. Rev. Lett. **83**, 2876 (1999).
[5] J. Steinhauer *et al.*, Phys. Rev. Lett. **88**, 120407 (2002).
[6] R. Ozeri *et al.*, Phys. Rev. Lett. **88**, 220401 (2002).
[7] N. Katz *et al.*, Phys. Rev. Lett. **89**, 220401 (2002).
[8] J. Hecker Denschlag *et al.*, J. Phys. B **35**, 3095 (2002).
[9] N. Katz *et al.*, Phys. Rev. A **70**, 033615 (2004).
[10] A. S. Mellish *et al.*, Phys. Rev. A **68**, 051601(R) (2003).
[11] O. Morsch *et al.*, Phys. Rev. Lett. **87**, 140402 (2001).
[12] F. Cataliotti *et al.*, Science **293**, 843 (2001).
[13] B. Anderson and M. Kasevich, Science **282**, 1686 (1998).
[14] M. Greiner *et al.*, Nature (London) **415**, 39 (2002).
[15] M. Kraemer *et al.*, Eur. Phys. J. D **27**, 247 (2003).
[16] D.-I. Choi and Q. Niu, Phys. Rev. Lett. **82**, 2022 (1999).
[17] D. Tannor, *Introduction to Quantum Mechanics: A Time-Dependent Perspective* (University Science Books, Sausalito, CA, 2005).
[18] We numerically solve the GPE for the order parameter of the condensate as described in [21], $i\hbar\partial_t\psi = \{-\hbar^2\nabla^2/2M + V + g|\psi|^2\}\psi$, with the time-dependent external potential typically of the form $V(\mathbf{r},t) = M/2(\omega_r^2 r^2 + \omega_z^2 z^2) + \hbar\Omega_d \cos(2k_L z - \omega_d t) + \hbar\Omega_p \cos(2k_L z - \omega_p t)$. The number of atoms in the simulation is 3×10^5. All other parameters for the simulation are as in the experimental system, described above. The ground state is found for $t=0$ by imaginary time evolution. We exploit the cylindrical symmetry to evolve the wave function on a two-dimensional grid $N_z \times N_r$ (4096×32), using the Crank-Nicholson differencing method with alternating direction implicit algorithm.
[19] E. Rowen *et al.*, e-print cond-mat/0506318.
[20] C. Cohen-Tannoudji *et al.*, *Atom-Photon Interactions* (John Wiley & Sons, New York, 1992).
[21] N. Katz *et al.*, e-print cond-mat/0505762.